




## ORGANIC CHEMISTRY

Article

Received: 10 May 2023 | Revised: 09 October 2023 |  
Accepted: 21 October 2023 | Published online: 15 November 2023

UDC 547; 544.18

<https://doi.org/10.31489/2959-0663/4-23-1>

Rahul K. Godge\* , Anurag K. Nalawade , Piyusha V. Kolhe 

Department of Pharmaceutical Chemistry, Pravara Rural College of Pharmacy Pravaranagar, Tal-Rahata,  
District-Ahmednagar, Maharashtra, India

(\*Corresponding author's e-mail: [rahulgodge@gmail.com](mailto:rahulgodge@gmail.com))

### Exploring the Antifungal Potential of 1,2,4-Triazole Derivatives: A Comprehensive Study on Design and Synthesis

Discovery of new antifungal agents is of great importance due to the increased prevalence of fungal infections and the emergence of drug-resistant strains. 1,2,4-Triazole derivatives have shown promising antifungal activity; therefore, this study aimed to design, synthesize and evaluate the antifungal potential of a series of 1,2,4-triazole derivatives. A series of 1,2,4-triazole derivatives were designed and synthesized. The compounds were characterized using FTIR, NMR and MS techniques. In silico studies including ADME properties, drug-likeness and molecular docking were carried out to evaluate the potential of the synthesized compounds as antifungal agents. In vitro antifungal activity was evaluated against *Candida albicans* and *Aspergillus niger* using the agar well diffusion method and zones of inhibition were measured. All synthesized compounds exhibited good physicochemical properties and drug-likeness profiles. Compounds AN5 and AN6 displayed the highest binding affinities of -9.2 and -10.0 kcal/mol, respectively, and showed promising antifungal activity. At a concentration of 100 µg/ml, compound AN5 exhibited zones of inhibition of 19.9 mm and 20.5 mm against *C. albicans* and *A. niger*, respectively, while compound AN6 displayed zones of inhibition of 19.5 mm and 22.5 mm, respectively. The marketed standard, namely itraconazole at the same concentration showed zones of inhibition of 23.8 mm and 24.7 mm. The designed 1,2,4-triazole derivatives, particularly AN5 and AN6, demonstrated promising antifungal activity against *C. albicans* and *A. niger*, making them potential candidates for further development as antifungal agents.

**Keywords:** 1,2,4-triazole derivatives, antifungal activity, in silico studies, molecular docking, *Candida albicans*, *Aspergillus niger*.

#### Abbreviation

FTIR: Fourier Transform Infrared Spectroscopy; NMR: Nuclear Magnetic Resonance Spectroscopy; MS: Mass Spectrometry; ADME: Absorption, Distribution, Metabolism and Excretion; CMC: Critical Micelle Concentration; TPSA: Topological Polar Surface Area; Papp: Apparent Permeability; GI: Gastrointestinal; BBB: Blood-Brain Barrier; PPB: Plasma Protein Binding; CYP: Cytochrome P450; PDB ID: Protein Data Bank Identifier; MS: Marketed Standard.

#### Introduction

Fungal infections have become a major global health problem, affecting millions of people each year. The increase in incidence can be attributed to several factors, including the growing number of immunocompromised individuals, the widespread use of antibiotics and the evolution of drug-resistant fungal strains [1]. Consequently, there is an urgent need for the development of novel antifungal agents with improved efficacy, safety and resistance profiles. Antifungal agents play a critical role in the treatment and prevention of fungal infections. They are used to treat superficial mycoses such as dermatophytosis and systemic mycoses,

namely invasive candidiasis and aspergillosis [1]. The availability of effective antifungal agents is of utmost importance because some fungal infections can result in severe morbidity and mortality if left untreated [2, 3].

The current arsenal of antifungal agents includes primarily four major classes: polyenes, azoles, echinocandins and allylamines. Among these, azole antifungals are the most widely used, owing to their broad spectrum of activity and relatively low toxicity. However, the widespread and prolonged use of azoles has led to the emergence of drug-resistant fungal strains, limiting the efficacy of these agents [4]. Moreover, existing antifungal drugs are also associated with various side effects, drug interactions and narrow therapeutic indices, further limiting their use. These limitations emphasize the urgent need for the discovery and development of new antifungal agents with novel mechanisms of action, improved safety profiles and reduced propensity for the development of resistance [5].

The 1,2,4-triazole scaffold has gained significant interest as a core structure for the development of new antifungal agents. 1,2,4-Triazoles are a class of heterocyclic compounds characterized by a five-membered ring containing three nitrogen atoms and two carbon atoms. The unique chemical properties of the 1,2,4-triazole scaffold, such as its ability to form strong hydrogen bonds and its high lipophilicity, make it an attractive candidate for drug development. Many 1,2,4-triazole derivatives have demonstrated promising antifungal activity, with some even surpassing the efficacy of existing azole antifungals. Fluconazole, itraconazole and voriconazole, all clinically used azole antifungals, possess the 1,2,4-triazole scaffold in their structure. This evidence further supports the potential of 1,2,4-triazole derivatives as effective antifungal agents [6, 7].

The development of novel 1,2,4-triazole derivatives as antifungal agents requires a systematic approach, combining rational design strategies, synthetic chemistry and biological evaluation. Rational drug design involves the modification of the core 1,2,4-triazole scaffold to introduce new functional groups, aiming to enhance antifungal activity, reduce toxicity and minimize the likelihood of resistance development [8]. Recent advances in computational chemistry, including molecular docking and quantitative structure-activity relationship (QSAR) studies, have facilitated the rational design of 1,2,4-triazole derivatives with optimized pharmacological profiles. These *in silico* tools allow researchers to predict the binding affinity and selectivity of the designed compounds for their target proteins, which facilitates the selection of promising candidates for synthesis and biological evaluation [9].

Synthetic chemistry plays a crucial role in the development of novel 1,2,4-triazole derivatives. Various synthetic routes and strategies have been employed to access a diverse range of 1,2,4-triazole derivatives with varied substitution patterns and functional groups. This diversity enables the exploration of structure-activity relationships (SAR) and the optimization of pharmacokinetic and pharmacodynamic properties [10].

Invasive fungal infections (IFIs) are increasingly becoming major infectious diseases worldwide, and the limited efficacy of existing drugs results in significant patient morbidity and mortality due to lack of effective antifungal agents and serious drug resistance. In this study, a series of benzimidazole-1,2,4-triazole derivatives (**6a-6l**) were synthesized and characterized by <sup>1</sup>H NMR and HR-MS spectral analysis. All the target compounds were screened for their *in vitro* antifungal activity against four fungal strains, namely *C. albicans*, *C. glabrata*, *C. krusei*, and *C. parapsilopsis*. The synthesized compounds exhibited significant antifungal potential, especially against *C. glabrata* [11].

With the above perspectives in mind, the primary purpose of our research work is to explore the potential of 1,2,4-triazole derivatives as a novel class of antifungal agents. Using the principles of rational drug design, synthetic chemistry and biological evaluation, we aim to develop new 1,2,4-triazole derivatives with enhanced antifungal activity, improved safety profiles and less propensity to develop resistance. This comprehensive study will not only expand our understanding of the structure-activity relationship (SAR) of 1,2,4-triazole derivatives but also help in developing innovative strategies to combat fungal infections. We anticipate that our findings will stimulate further research in this field and pave the way for the development of next-generation antifungal agents.

## Experimental

### Materials

All chemicals and reagents required for the synthesis of 1,2,4-triazole derivatives were procured from the stores of Pravara Rural College of Pharmacy, India. The reference compound, itraconazole, was obtained from Sciquaint Innovations (OPC) Private Limited, Pune. Solvents and other materials used in the study were of analytical grade and used without further purification unless otherwise stated. Fourier Transform

Infrared Spectroscopy (FTIR) spectra of the synthesized compounds were recorded on a Bruker eco FTIR spectrometer using the KBr pellet technique. Proton Nuclear Magnetic Resonance ( $^1\text{H}$  NMR) spectra were obtained on a Bruker eco spectrometer operating at 400 MHz using deuterated dimethyl sulfoxide (DMSO- $d_6$ ) as a solvent and tetramethylsilane (TMS) as an internal standard. Chemical shifts were reported in parts per million (ppm). Melting points of the synthesized compounds were determined using a digital Gallen Kemp melting point apparatus and were uncorrected.

#### Molecular Docking

Molecular docking studies were performed using AutoDock Vina software to evaluate the binding affinity and interaction patterns of the synthesized 1,2,4-triazole derivatives with the target protein. The X-ray crystal structure of the target protein (PDB ID: 5EQB) was retrieved from the Protein Data Bank and prepared for docking studies using the Discovery Studio Visualizer. Hydrogen atoms and Kollman charges were added, and water molecules were removed. The ligands were drawn using ChemDraw and optimized with Chem3D before being converted to PDBQT format using AutoDockTools. The docking grid was defined to encompass the active site of the protein, and the exhaustiveness parameter was set to 8. The best docked poses were selected based on their binding affinity scores, and the protein-ligand interactions were visualized and analyzed using LigPlot+ and Discovery Studio Visualizer [12, 13].

#### In Silico ADMET Prediction

In silico ADMET (Absorption, Distribution, Metabolism, Excretion and Toxicity) properties of the synthesized 1,2,4-triazole derivatives were predicted using SwissADME and PreADMET web-based tools. The SMILES notation of each compound was input into the respective servers and the predicted ADMET properties including gastrointestinal absorption, blood-brain barrier penetration and cytochrome P450 inhibition were obtained. These predictions provide valuable insights into the pharmacokinetic profile of the synthesized compounds and their potential as drug candidates [14].

#### Lipinski's Rule of Five and Drug-likeness Analysis

The drug-likeness of the synthesized 1,2,4-triazole derivatives was evaluated based on Lipinski's Rule of Five, which is a set of criteria used to predict the oral bioavailability of compounds. The rule states that a compound is likely to be orally bioavailable if it has: (1) no more than 5 hydrogen bond donors, (2) no more than 10 hydrogen bond acceptors, (3) a molecular weight less than 500 Da and (4) a calculated logP (partition coefficient) value less than 5. The Lipinski's Rule of Five parameters were calculated using SwissADME and PreADMET, and compounds satisfying these criteria were considered as having favourable drug-likeness properties [15, 16].

#### Synthesis and Spectral Analysis of Synthesized Compounds

Figure 1 presents proposed scheme of synthesis of 1,2,4-triazole derivatives. Designed derivatives of 1,2,4-triazole listed in Table 1.

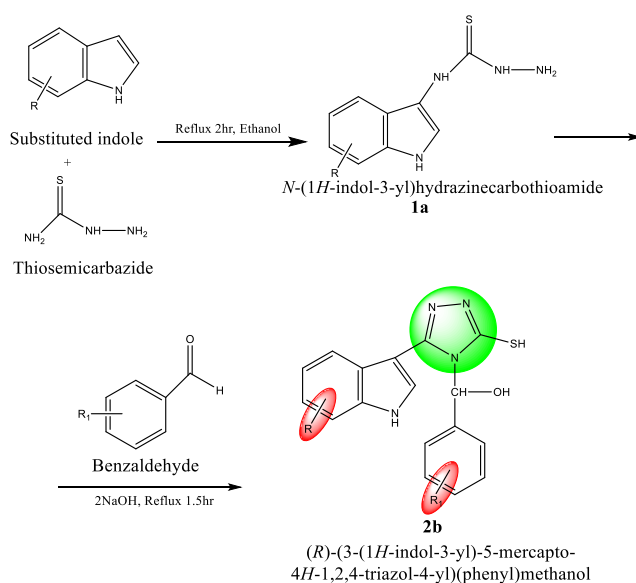


Figure 1. Proposed scheme of synthesis of 1,2,4-triazole derivatives

Designed derivatives of 1,2,4-triazole

Sr. No.	Label	R	R <sub>1</sub>
1	AN1	-Cl	-CH <sub>3</sub>
2	AN2	-CH <sub>3</sub>	-H
3	AN3	-NO <sub>2</sub>	-Cl
4	AN4	-C <sub>2</sub> H <sub>5</sub>	-H
5	AN5	-H	-C <sub>2</sub> H <sub>5</sub>
6	AN6	-Br	-NO <sub>2</sub>
7	AN7	-OCH <sub>3</sub>	-H
8	AN8	-H	-OCH <sub>3</sub>
9	AN9	-F	-H
10	AN10	-CH <sub>3</sub>	-Br

**Synthesis of (R)-(3-(6-chloro-1H-indol-3-yl)-5-mercapto-4H-1,2,4-triazol-4-yl)(p-tolyl)methanol (AN1)** [17]. A mixture of *para*-chloroindole (1.0 mmol) and thiosemicarbazide (1.0 mmol) in ethanol (10 mL) was stirred at room temperature for 2 hours. After completion of the reaction, the reaction mixture was cooled; the precipitate was collected, washed with cold ethanol and dried. The melting point was recorded. The product was then reacted with *para*-methylbenzaldehyde (1.0 mmol) in ethanol (10 mL) in the presence of sodium hydroxide (2.0 mmol). The mixture was stirred at room temperature for 1.5 hours, cooled; the precipitate was collected, washed with cold ethanol, dried and the melting point was recorded.

Orange Solid, **Yield:** 74 %, **M.p.** 178-182 °C, **Rf value:** 0.72, **FTIR (cm<sup>-1</sup>):** 3402.72 cm<sup>-1</sup> (O-H stretching of the alcohol group), 3104.31 cm<sup>-1</sup> and 3049.33 cm<sup>-1</sup> (Aromatic C-H stretching), 1891.51 cm<sup>-1</sup> (C=N stretching), 1808.67 cm<sup>-1</sup>, 1615.40 cm<sup>-1</sup>, and 1590.92 cm<sup>-1</sup> (C=C stretching of the aromatic ring), 1775.86 cm<sup>-1</sup> and 1694.93 cm<sup>-1</sup> (C=O stretching), 1487.40 cm<sup>-1</sup>, 1452.29 cm<sup>-1</sup>, and 1410.32 cm<sup>-1</sup> (C=C bending of the aromatic ring), 1332.71 cm<sup>-1</sup> (N-H bending), 1274.98 cm<sup>-1</sup>, 1241.31 cm<sup>-1</sup>, 1203.74 cm<sup>-1</sup>, 1120.11 cm<sup>-1</sup>, 1089.24 cm<sup>-1</sup>, 1058.36 cm<sup>-1</sup>, and 1006.99 cm<sup>-1</sup> (C-N stretching), 929.96 cm<sup>-1</sup> and 893.47 cm<sup>-1</sup> (C-H bending of the aromatic ring), 821.07 cm<sup>-1</sup> and 608.44 cm<sup>-1</sup> (Triazole ring), 740.85 cm<sup>-1</sup> (C-Cl stretching), and 580.20 cm<sup>-1</sup> (C-S stretching), 514.91 cm<sup>-1</sup> (Toluene ring), **<sup>1</sup>H NMR (δppm):** 8.03 d Ar-H (Indole), 7.63 d Ar-H (Triazole), 7.62 d Ar-H (*p*-Tolyl), 7.60 — 7.33 m Ar-H (Indole), 7.31 — 7.22 m Ar-H (*p*-Tolyl), 7.21-6.65 dd Ar-H (Indole), 2.89-2.86 s OH (Methanol), 2.71-2.68 t CH<sub>3</sub> (*p*-Tolyl).

**Synthesis of (R)-(3-mercapto-5-(6-methyl-1H-indol-3-yl)-4H-1,2,4-triazol-4-yl)(phenyl)methanol (AN2).** A mixture of *para*-methylindole (1.0 mmol) and thiosemicarbazide (1.0 mmol) in ethanol (10 mL) was stirred at room temperature for 2 hours. After completion of the reaction, the reaction mixture was cooled; the precipitate was collected, washed with cold ethanol and dried. The melting point was recorded. The product was then reacted with benzaldehyde (1.0 mmol) in ethanol (10 mL) in the presence of sodium hydroxide (2.0 mmol). The mixture was stirred at room temperature for 1.5 hours, cooled, the precipitate was collected, washed with cold ethanol, dried and the melting point was recorded.

Brown Solid, **Yield:** 85 %, **M.p.** 171-175 °C, **Rf value:** 0.83, **FTIR (cm<sup>-1</sup>):** 3382.77 cm<sup>-1</sup> (O-H stretching of the alcohol group), 3148.49 cm<sup>-1</sup>, 3064.97 cm<sup>-1</sup>, 3017.19 cm<sup>-1</sup>, 2943.59 cm<sup>-1</sup>, and 2854.36 cm<sup>-1</sup> (Aromatic C-H stretching), 2113.05 cm<sup>-1</sup>, 1987.07 cm<sup>-1</sup>, and 1921.98 cm<sup>-1</sup> (C≡N stretching), 1692.79 cm<sup>-1</sup> (C=O stretching), 1661.78 cm<sup>-1</sup>, 1586.39 cm<sup>-1</sup>, and 1507.36 cm<sup>-1</sup> (C=C stretching of the aromatic ring), 1458.77 cm<sup>-1</sup> (C=C bending of the aromatic ring), 1426.67 cm<sup>-1</sup>, 1371.41 cm<sup>-1</sup> (C-H bending of the aromatic ring), 1297.13 cm<sup>-1</sup>, 1263.69 cm<sup>-1</sup>, 1199.85 cm<sup>-1</sup>, 1150.57 cm<sup>-1</sup>, and 1119.98 cm<sup>-1</sup> (C-N stretching), 1024.08 cm<sup>-1</sup> (C-H bending of the aromatic ring), 858.31 cm<sup>-1</sup>, 811.19 cm<sup>-1</sup>, and 628.67 cm<sup>-1</sup> (Triazole ring), 751.64 cm<sup>-1</sup> (C-S stretching), 727.49 cm<sup>-1</sup> (Toluene ring), 585.43 cm<sup>-1</sup>, and 547.01 cm<sup>-1</sup> (C-H bending of the aromatic ring). **<sup>1</sup>H NMR (δppm):** 8.02 d Ar-H (Indole), 7.63 d Ar-H (Triazole), 7.56 dd Ar-H (*p*-Tolyl), 7.50-7.40 m Ar-H (Indole), 7.34-7.27 m Ar-H (*p*-Tolyl), 7.19 dd Ar-H (Triazole), 2.98-2.95 s OH (Methanol), 2.73-2.69 t CH<sub>3</sub> (*p*-Tolyl).

**Synthesis of (R)-(4-chlorophenyl)(3-mercapto-5-(6-nitro-1H-indol-3-yl)-4H-1,2,4-triazol-4-yl)-methanol (AN3).** A mixture of *para*-nitroindole (1.0 mmol) and thiosemicarbazide (1.0 mmol) in ethanol (10 mL) was stirred at room temperature for 2 hours. After completion of the reaction, the reaction mixture was cooled; the precipitate was collected, washed with cold ethanol and dried. The melting point was recorded. The product was then reacted with *para*-chlorobenzaldehyde (1.0 mmol) in ethanol (10 mL) in the

presence of sodium hydroxide (2.0 mmol). The mixture was stirred at room temperature for 1.5 hours, cooled, the precipitate was collected, washed with cold ethanol, dried and the melting point was recorded.

Brown Solid, **Yield:** 67 %, **M.p.** 184–188 °C, **Rf value:** 0.63, **FTIR (cm<sup>-1</sup>):** 3380.14 cm<sup>-1</sup> (O-H stretching of the alcohol group), 3146.56 cm<sup>-1</sup>, 3061.03 cm<sup>-1</sup>, 3007.82 cm<sup>-1</sup>, 2962.94 cm<sup>-1</sup>, 2945.90 cm<sup>-1</sup>, 2918.81 cm<sup>-1</sup>, and 2848.72 cm<sup>-1</sup> (Aromatic C-H stretching), 2732.54 cm<sup>-1</sup>, and 2113.99 cm<sup>-1</sup> (C≡N stretching), 2662.16 cm<sup>-1</sup> (C-H bending of the aromatic ring), 2570.99 cm<sup>-1</sup> (NO<sub>2</sub> stretching), 1875.34 cm<sup>-1</sup> and 1692.74 cm<sup>-1</sup> (C=O stretching), 1810.32 cm<sup>-1</sup>, 1719.79 cm<sup>-1</sup>, 1661.16 cm<sup>-1</sup>, 1587.52 cm<sup>-1</sup>, and 1507.49 cm<sup>-1</sup> (C=C stretching of the aromatic ring), 1460.61 cm<sup>-1</sup> (C=C bending of the aromatic ring), 1427.36 cm<sup>-1</sup>, 1371.59 cm<sup>-1</sup> (C-H bending of the aromatic ring), 1334.06 cm<sup>-1</sup> (N-H bending), 1297.60 cm<sup>-1</sup>, 1265.85 cm<sup>-1</sup>, 1203.91 cm<sup>-1</sup>, 1152.67 cm<sup>-1</sup>, and 1120.66 cm<sup>-1</sup> (C-N stretching), 1026.27 cm<sup>-1</sup> (C-H bending of the aromatic ring), 895.48 cm<sup>-1</sup>, 862.66 cm<sup>-1</sup>, and 819.80 cm<sup>-1</sup> (Triazole ring), 750.91 cm<sup>-1</sup> (C-S stretching), 726.52 cm<sup>-1</sup> (Toluene ring), 628.87 cm<sup>-1</sup> (Triazole ring), 585.47 cm<sup>-1</sup>, and 542.07 cm<sup>-1</sup> (C-H bending of the aromatic ring), **NMR (δppm):** 8.03 d Ar-H (Indole), 7.63 d Ar-H (Triazole), 7.56 d Ar-H (*p*-Tolyl), 7.50–7.40 m Ar-H (Indole), 7.34–7.27 m Ar-H (*p*-Tolyl), 7.19 dd Ar-H (Triazole), 2.96–2.94 s OH (Methanol), 2.73–2.70 t CH<sub>3</sub> (*p*-Tolyl).

**Synthesis of (R)-(3-(6-ethyl-1H-indol-3-yl)-5-mercapto-4H-1,2,4-triazol-4-yl)(phenyl)methanol (AN4).** A mixture of *para*-ethylindole (1.0 mmol) and thiosemicarbazide (1.0 mmol) in ethanol (10 mL) was stirred at room temperature for 2 hours. After completion of the reaction, the reaction mixture was cooled; the precipitate was collected, washed with cold ethanol and dried. The melting point was recorded. The product was then reacted with benzaldehyde (1.0 mmol) in ethanol (10 mL) in the presence of sodium hydroxide (2.0 mmol). The mixture was stirred at room temperature for 1.5 hours, cooled; the precipitate was collected, washed with cold ethanol, dried and the melting point was recorded.

Brown Solid, **Yield:** 76 %, **M.p.** 173–176 °C, **Rf value:** 0.79, **FTIR (cm<sup>-1</sup>):** 3428.02 cm<sup>-1</sup> (O-H stretching of the alcohol group), 3323.06 cm<sup>-1</sup> (N-H stretching), 3090.07 cm<sup>-1</sup>, 3056.04 cm<sup>-1</sup>, 2970.75 cm<sup>-1</sup>, and 2840.19 cm<sup>-1</sup> (Aromatic C-H stretching), 2138.27 cm<sup>-1</sup> (C≡N stretching), 1912.30 cm<sup>-1</sup> (C=O stretching), 1661.89 cm<sup>-1</sup>, 1584.73 cm<sup>-1</sup>, and 1533.63 cm<sup>-1</sup> (C=C stretching of the aromatic ring), 1486.50 cm<sup>-1</sup> (C=C bending of the aromatic ring), 1457.32 cm<sup>-1</sup>, and 1385.33 cm<sup>-1</sup> (C-H bending of the aromatic ring), 1287.92 cm<sup>-1</sup>, 1204.25 cm<sup>-1</sup>, 1152.15 cm<sup>-1</sup>, 1124.94 cm<sup>-1</sup>, 1087.35 cm<sup>-1</sup>, and 1008.94 cm<sup>-1</sup> (C-N stretching), 865.08 cm<sup>-1</sup>, 817.61 cm<sup>-1</sup>, and 789.25 cm<sup>-1</sup> (Triazole ring), 741.23 cm<sup>-1</sup> (C-S stretching), 626.44 cm<sup>-1</sup> (Triazole ring), 593.39 cm<sup>-1</sup>, and 547.82 cm<sup>-1</sup> (C-H bending of the aromatic ring), **<sup>1</sup>H NMR (δppm):** 8.03 d Ar-H (Indole), 7.63 d Ar-H (Triazole), 7.51 d Ar-H (Phenyl), 7.48–7.36 m Ar-H (Indole), 7.27–7.20 m Ar-H (Phenyl), 7.18 dd Ar-H (Triazole), 2.96–2.93 s OH (Alcohol), 2.72–2.69 t CH<sub>3</sub> (Phenyl).

**Synthesis of (R)-(3-(1H-indol-3-yl)-5-mercapto-4H-1,2,4-triazol-4-yl)(4-ethylphenyl)methanol (AN5).** A mixture of indole (1.0 mmol) and thiosemicarbazide (1.0 mmol) in ethanol (10 mL) was stirred at room temperature for 2 hours. After completion of the reaction, the reaction mixture was cooled; the precipitate was collected, washed with cold ethanol and dried. The melting point was recorded. The product was then reacted with *para*-ethylbenzaldehyde (1.0 mmol) in ethanol (10 mL) in the presence of sodium hydroxide (2.0 mmol). The mixture was stirred at room temperature for 1.5 hours, cooled; the precipitate was collected, washed with cold ethanol, dried and the melting point was recorded.

Orange Solid, **Yield:** 66 %, **M.p.** 176–179 °C, **Rf value:** 0.65, **MS (m/e):** 350.44, **FTIR (cm<sup>-1</sup>):** 3427.55 cm<sup>-1</sup> (O-H stretching of the alcohol group), 3327.72 cm<sup>-1</sup> and 3256.93 cm<sup>-1</sup> (N-H stretching), 2838.15 cm<sup>-1</sup> (Aromatic C-H stretching), 1678.91 cm<sup>-1</sup> and 1587.89 cm<sup>-1</sup> (C=C stretching of the aromatic ring), 1455.85 cm<sup>-1</sup> and 1360.65 cm<sup>-1</sup> (C-H bending of the aromatic ring), 1284.21 cm<sup>-1</sup>, 1204.36 cm<sup>-1</sup>, 1150.45 cm<sup>-1</sup>, 1086.91 cm<sup>-1</sup>, and 1006.75 cm<sup>-1</sup> (C-N stretching), 932.38 cm<sup>-1</sup>, 819.19 cm<sup>-1</sup>, and 785.80 cm<sup>-1</sup> (Triazole ring), 741.30 cm<sup>-1</sup> (C-S stretching), 639.29 cm<sup>-1</sup> (Triazole ring), 614.98 cm<sup>-1</sup>, and 548.97 cm<sup>-1</sup> (C-H bending of the aromatic ring), **<sup>1</sup>H NMR (δppm):** 8.03 d Ar-H (Indole), 7.64 d Ar-H (Triazole), 7.46 d Ar-H (*p*-Ethylphenyl), 7.44–7.31 m Ar-H (Indole), 7.29–7.21 m Ar-H (*p*-Ethylphenyl), 7.17 dd Ar-H (Triazole), 2.93–2.91 s OH (Alcohol), 2.67–2.64 t CH<sub>3</sub> (*p*-Ethylphenyl).

**Synthesis of (R)-(3-(6-bromo-1H-indol-3-yl)-5-mercapto-4H-1,2,4-triazol-4-yl)(4-nitrophenyl)methanol (AN6).** A mixture of *para*-bromoindole (1.0 mmol) and thiosemicarbazide (1.0 mmol) in ethanol (10 mL) was stirred at room temperature for 2 hours. After completion of the reaction, the reaction mixture was cooled; the precipitate was collected, washed with cold ethanol and dried. The melting point was recorded. The product was then reacted with *para*-nitrobenzaldehyde (1.0 mmol) in ethanol (10 mL) in the presence of sodium hydroxide (2.0 mmol). The mixture was stirred at room temperature for 1.5 hours, cooled; the precipitate was collected, washed with cold ethanol, dried and the melting point was recorded.

Brown solid, **Yield:** 73 %, **M.p.** 183-186 °C, **Rf value:** 0.78, **MS (m/e):** 446.38, **FTIR (cm<sup>-1</sup>):** 3435.10 cm<sup>-1</sup> (O-H stretching of the alcohol group), 3323.82 cm<sup>-1</sup> (N-H stretching), 3138.86 cm<sup>-1</sup> and 2789.10 cm<sup>-1</sup> (Aromatic C-H stretching), 2189.43 cm<sup>-1</sup>, 2103.72 cm<sup>-1</sup>, and 2014.23 cm<sup>-1</sup> (C≡N stretching), 1846.17 cm<sup>-1</sup> (C=O stretching), 1808.25 cm<sup>-1</sup>, 1655.05 cm<sup>-1</sup>, and 1586.80 cm<sup>-1</sup> (C=C stretching of the aromatic ring), 1460.26 cm<sup>-1</sup> and 1401.64 cm<sup>-1</sup> (C=C bending of the aromatic ring), 1134.84 cm<sup>-1</sup> and 1004.18 cm<sup>-1</sup> (C-N stretching), 955.77 cm<sup>-1</sup> (NO<sub>2</sub> stretching), 784.78 cm<sup>-1</sup> (Triazole ring), 705.64 cm<sup>-1</sup> and 675.88 cm<sup>-1</sup> (Triazole ring), 626.44 cm<sup>-1</sup> (C-S stretching), 562.81 cm<sup>-1</sup> and 514.92 cm<sup>-1</sup> (C-H bending of the aromatic ring), **<sup>1</sup>H NMR (δppm):** 8.05 d Ar-H (Indole), 7.63 d Ar-H (Triazole), 7.48 d Ar-H (p-Nitrophenyl), 7.45-7.33 m Ar-H (Indole), 7.28-7.21 m Ar-H (p-Nitrophenyl), 7.18 dd Ar-H (Triazole), 2.94-2.92 s OH (Alcohol), 2.68-2.65 t CH<sub>3</sub> (p-Nitrophenyl).

**Synthesis of (R)-(3-mercapto-5-(6-methoxy-1H-indol-3-yl)-4H-1,2,4-triazol-4-yl)(phenyl) methanol (AN7).** A mixture of *para*-methoxyindole (1.0 mmol) and thiosemicarbazide (1.0 mmol) in ethanol (10 mL) was stirred at room temperature for 2 hours. After completion of the reaction, the reaction mixture was cooled; the precipitate was collected, washed with cold ethanol and dried. The melting point was recorded. The product was then reacted with benzaldehyde (1.0 mmol) in ethanol (10 mL) in the presence of sodium hydroxide (2.0 mmol). The mixture was stirred at room temperature for 1.5 hours, cooled; the precipitate was collected, washed with cold ethanol, dried and the melting point was recorded.

Brown Solid, **Yield:** 87 %, **M.p.** 174-178 °C, **Rf value:** 0.89, **FTIR (cm<sup>-1</sup>):** 3530.73 cm<sup>-1</sup> (O-H stretching of the alcohol group), 3428.23 cm<sup>-1</sup> and 3330.12 cm<sup>-1</sup> (N-H stretching), 3132.46 cm<sup>-1</sup> and 2879.32 cm<sup>-1</sup> (Aromatic C-H stretching), 2637.87 cm<sup>-1</sup> and 2487.75 cm<sup>-1</sup> (C-H bending of the aromatic ring), 2595.84 cm<sup>-1</sup>, 2209.76 cm<sup>-1</sup>, and 2095.42 cm<sup>-1</sup> (C≡N stretching), 1944.78 cm<sup>-1</sup> (C=O stretching), 1735.54 cm<sup>-1</sup>, 1684.95 cm<sup>-1</sup>, 1624.49 cm<sup>-1</sup>, and 1528.69 cm<sup>-1</sup> (C=C stretching of the aromatic ring), 1493.16 cm<sup>-1</sup> (C=C bending of the aromatic ring), 1466.38 cm<sup>-1</sup> and 1417.02 cm<sup>-1</sup> (C-H bending of the aromatic ring), 1327.29 cm<sup>-1</sup> and 1287.09 cm<sup>-1</sup> (C-N stretching), 1190.50 cm<sup>-1</sup> (C-O stretching), 1137.98 cm<sup>-1</sup> and 1007.91 cm<sup>-1</sup> (C-N stretching), 936.13 cm<sup>-1</sup>, 903.61 cm<sup>-1</sup>, and 856.67 cm<sup>-1</sup> (Triazole ring), 736.57 cm<sup>-1</sup>, 702.38 cm<sup>-1</sup>, and 660.17 cm<sup>-1</sup> (C-H bending of the aromatic ring), 550.15 cm<sup>-1</sup> (C-H bending of the aromatic ring), **<sup>1</sup>H NMR (δppm):** 7.28-7.26 m Ar-H (Indole), 7.22-7.21 m Ar-H (*p*-Tolyl), 7.20-7.17 dd Ar-H (Indole), 7.15-7.12 dd Ar-H (Indole), 7.10-7.06 m Ar-H (Indole), 3.91-3.88 s OH (Methanol), 2.70-2.67 t CH<sub>3</sub> (*p*-Tolyl).

**Synthesis of (R)-(3-(1H-indol-3-yl)-5-mercapto-4H-1,2,4-triazol-4-yl)(4-methoxyphenyl) methanol (AN8).** A mixture of indole (1.0 mmol) and thiosemicarbazide (1.0 mmol) in ethanol (10 mL) was stirred at room temperature for 2 hours. After completion of the reaction, the reaction mixture was cooled; the precipitate was collected, washed with cold ethanol and dried. The melting point was recorded. The product was then reacted with *para*-methoxybenzaldehyde (1.0 mmol) in ethanol (10 mL) in the presence of sodium hydroxide (2.0 mmol). The mixture was stirred at room temperature for 1.5 hours, cooled and the precipitate was collected, washed with cold ethanol, dried and the melting point was recorded.

Orange Solid, **Yield:** 79 %, **M.p.** 178-183 °C, **Rf value:** 0.71, **FTIR (cm<sup>-1</sup>):** 3472.91 cm<sup>-1</sup> (O-H stretching of the alcohol group), 3342.49 cm<sup>-1</sup> (N-H stretching), 3165.26 cm<sup>-1</sup>, 2942.89 cm<sup>-1</sup>, 2915.32 cm<sup>-1</sup>, and 2887.85 cm<sup>-1</sup> (Aromatic C-H stretching), 2597.58 cm<sup>-1</sup>, 2513.43 cm<sup>-1</sup>, 2440.80 cm<sup>-1</sup>, 2405.11 cm<sup>-1</sup>, and 2352.02 cm<sup>-1</sup> (C-H bending of the aromatic ring), 2221.97 cm<sup>-1</sup> (C≡N stretching), 2093.47 cm<sup>-1</sup> and 2015.86 cm<sup>-1</sup> (C=C stretching of the aromatic ring), 1956.42 cm<sup>-1</sup> (C=O stretching), 1623.09 cm<sup>-1</sup>, 1598.15 cm<sup>-1</sup>, 1565.87 cm<sup>-1</sup>, and 1496.88 cm<sup>-1</sup> (C=C stretching of the aromatic ring), 1468.24 cm<sup>-1</sup> (C=C bending of the aromatic ring), 1424.21 cm<sup>-1</sup> (C-H bending of the aromatic ring), 1340.96 cm<sup>-1</sup> and 1283.83 cm<sup>-1</sup> (C-N stretching), 1235.11 cm<sup>-1</sup> (C-O stretching), 1160.86 cm<sup>-1</sup>, 1095.89 cm<sup>-1</sup>, and 1008.87 cm<sup>-1</sup> (C-N stretching), 935.87 cm<sup>-1</sup>, 905.14 cm<sup>-1</sup>, and 855.69 cm<sup>-1</sup> (Triazole ring), 777.52 cm<sup>-1</sup>, 736.26 cm<sup>-1</sup>, 697.81 cm<sup>-1</sup>, 659.29 cm<sup>-1</sup>, 595.48 cm<sup>-1</sup>, 552.69 cm<sup>-1</sup>, 519.44 cm<sup>-1</sup>, and 510.53 cm<sup>-1</sup> (C-H bending of the aromatic ring), **NMR (δ ppm):** 7.60 d Ar-H (Indole), 7.57 d Ar-H (Triazole), 7.53 d Ar-H (*p*-Methoxyphenyl), 7.43-7.35 m Ar-H (Indole), 7.28-7.25 m Ar-H (*p*-Methoxyphenyl), 7.25-7.20 m Ar-H (*p*-Methoxyphenyl), 7.20-7.17 m Ar-H (Indole), 7.15-7.12 m Ar-H (Indole), 3.98-3.95 s OH (Methanol), 3.84 s Ar-O-CH<sub>3</sub>, 2.82-2.79 t CH<sub>3</sub> (*p*-Methoxyphenyl).

**Synthesis of (R)-(3-(6-fluoro-1H-indol-3-yl)-5-mercapto-4H-1,2,4-triazol-4-yl)(phenyl)methanol (AN9).** A mixture of *para*-fluoroindole (1.0 mmol) and thiosemicarbazide (1.0 mmol) in ethanol (10 mL) was stirred at room temperature for 2 hours. After completion of the reaction, the reaction mixture was cooled; the precipitate was collected, washed with cold ethanol and dried. The melting point was recorded. The product was then reacted with benzaldehyde (1.0 mmol) in ethanol (10 mL) in the presence of sodium

hydroxide (2.0 mmol). The mixture was stirred at room temperature for 1.5 hours, cooled and the precipitate was collected, washed with cold ethanol, dried and the melting point was recorded.

Brown Solid, **Yield:** 83 %, **M.p.** 186-190 °C, **Rf value:** 0.85, **FTIR (cm<sup>-1</sup>):** 3402.72 cm<sup>-1</sup> (O-H stretching of the alcohol group), 3104.31 cm<sup>-1</sup> (N-H stretching), 3049.33 cm<sup>-1</sup> (Aromatic C-H stretching), 1891.51 cm<sup>-1</sup> (C=O stretching), 1808.67 cm<sup>-1</sup>, 1775.86 cm<sup>-1</sup>, 1694.93 cm<sup>-1</sup>, 1615.40 cm<sup>-1</sup>, 1590.92 cm<sup>-1</sup>, and 1487.40 cm<sup>-1</sup> (C=C stretching of the aromatic ring), 1452.29 cm<sup>-1</sup> (C=C bending of the aromatic ring), 1410.32 cm<sup>-1</sup> (C-H bending of the aromatic ring), 1332.71 cm<sup>-1</sup> and 1274.98 cm<sup>-1</sup> (C-N stretching), 1241.31 cm<sup>-1</sup> (C-O stretching), 1203.74 cm<sup>-1</sup>, 1120.11 cm<sup>-1</sup>, 1089.24 cm<sup>-1</sup>, and 1058.36 cm<sup>-1</sup> (C-N stretching), 1006.99 cm<sup>-1</sup> (C-N stretching), 929.96 cm<sup>-1</sup>, 893.47 cm<sup>-1</sup>, and 821.07 cm<sup>-1</sup> (Triazole ring), 740.85 cm<sup>-1</sup>, 608.44 cm<sup>-1</sup>, 580.20 cm<sup>-1</sup>, and 514.91 cm<sup>-1</sup> (C-H bending of the aromatic ring), **<sup>1</sup>H NMR (δppm):** 8.03 d Ar-H (Indole), 7.74 d Ar-H (Triazole), 7.69 d Ar-H (Phenyl), 7.57-7.52 dd Ar-H (Indole), 7.42-7.38 m Ar-H (Indole), 7.29-7.23 m Ar-H (Phenyl), 7.16-7.11 dd Ar-H (Indole), 3.95-3.92 s OH (Methanol).

**Synthesis of (R)-(4-bromophenyl)(3-mercapto-5-(6-methyl-1H-indol-3-yl)-4H-1,2,4-triazol-4-yl)-methanol (AN10).** A mixture of *para*-methylindole (1.0 mmol) and thiosemicarbazide (1.0 mmol) in ethanol (10 mL) was stirred at room temperature for 2 hours. After completion of the reaction, the reaction mixture was cooled; the precipitate was collected, washed with cold ethanol and dried. The melting point was recorded. The product was then reacted with *para*-bromobenzaldehyde (1.0 mmol) in ethanol (10 mL) in the presence of sodium hydroxide (2.0 mmol). The mixture was stirred at room temperature for 1.5 hours, cooled and the precipitate was collected, washed with cold ethanol, dried and the melting point was recorded.

Orange Solid, **Yield:** 85 %, **M.p.** 191-194 °C, **Rf value:** 0.83, **FTIR (cm<sup>-1</sup>):** 3427.55 cm<sup>-1</sup> (O-H stretching of the alcohol group), 3327.72 cm<sup>-1</sup> (N-H stretching), 3256.93 cm<sup>-1</sup> (Aromatic C-H stretching), 2838.15 cm<sup>-1</sup> (Aromatic C-H stretching), 1678.91 cm<sup>-1</sup> (C=O stretching), 1587.89 cm<sup>-1</sup> and 1455.85 cm<sup>-1</sup> (C=C stretching of the aromatic ring), 1360.65 cm<sup>-1</sup> (C-H bending of the aromatic ring), 1284.21 cm<sup>-1</sup>, 1204.36 cm<sup>-1</sup>, 1150.45 cm<sup>-1</sup>, 1086.91 cm<sup>-1</sup>, and 1006.75 cm<sup>-1</sup> (C-N stretching), 932.38 cm<sup>-1</sup>, 819.19 cm<sup>-1</sup>, and 785.80 cm<sup>-1</sup> (Triazole ring), 741.30 cm<sup>-1</sup>, 639.29 cm<sup>-1</sup>, 614.98 cm<sup>-1</sup>, and 548.97 cm<sup>-1</sup> (C-H bending of the aromatic ring), **<sup>1</sup>H NMR (δppm):** 8.03 d Ar-H (Indole), 7.63 d Ar-H (Triazole), 7.62 d Ar-H (*p*-Bromophenyl), 7.60-7.33 m Ar-H (Indole), 7.31-7.22 m Ar-H (*p*-Bromophenyl), 7.21-6.65 dd Ar-H (Indole), 2.89-2.86 s OH (Methanol), 2.71-2.68 t CH<sub>3</sub> (*p*-Bromophenyl).

#### *In Vitro* Antifungal activity

The *in vitro* antifungal activity of the synthesized compounds (AN1-AN10) was evaluated against *Candida albicans* and *Aspergillus niger* using the microdilution method. The microorganisms were cultured in Sabouraud dextrose broth and incubated for 24 hours at 37 °C [18]. The culture was then diluted to obtain a concentration of 1 × 10<sup>6</sup> colony-forming units per milliliter (CFU/mL). A serial dilution was performed for each compound to obtain concentrations ranging from 3.125 µg/mL to 200 µg/mL [19]. The microdilution plates were inoculated with 100 µL of the fungal suspension and 100 µL of the respective compound dilution. The final concentration of the fungal suspension in each well was 0.5 × 10<sup>6</sup> CFU/mL. Amphotericin B was used as a positive control and DMSO was used as a negative control. The plates were incubated at 37 °C for 24 hours. The minimum inhibitory concentration (MIC) was determined as the lowest concentration of the compound that inhibited the visible growth of the microorganism. The MIC values were recorded for each compound against both *Candida albicans* and *Aspergillus niger* at concentrations of 25, 50 and 100 µg/mL. The experiment was performed in triplicate and the results were reported as the mean ± standard deviation [19-21].

## Results and Discussion

### Chemistry

The compound described, (R)-(3-(1H-indol-3-yl)-5-mercapto-4H-1,2,4-triazol-4-yl)(phenyl)methanol, belongs to the 1,2,4-triazole class of derivatives (Fig. 2). The compound features a 1,2,4-triazole ring attached to an indole and a phenyl ring through a methylene bridge. The indole and phenyl rings have substituents R and R<sub>1</sub>, respectively. The presence of these substituents provides a wide range of potential chemical properties and biological activity.

The 1,2,4-triazole core is known for its versatile chemical reactivity and biological activities, which include antifungal, antibacterial, antiviral and anticancer properties. The indole ring is a common motif in natural products and pharmaceuticals, as it is a key component in several biologically active alkaloids. The phenyl ring further enhances the structural diversity and potential bioactivity of the molecule. The presence of



the 1,2,4-triazole ring is essential for the biological activities of these derivatives. This heterocyclic moiety is known for its versatile chemical reactivity and a wide range of biological activities, including antifungal properties. The nitrogen atoms in the triazole ring can form hydrogen bonds with active site residues of the target enzyme, contributing to the binding affinity and overall activity [22].

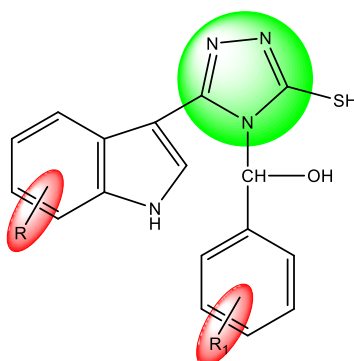


Figure 2. Chemistry of (R)-(3-(1H-indol-3-yl)-5-mercapto-4H-1,2,4-triazol-4-yl)(phenyl)methanol (AN)

The R substituents on the indole ring can affect the lipophilicity, electronic properties and steric hindrance of the molecules. These factors may influence the compound's ability to penetrate fungal cell membranes and interact with the target enzyme. For example, electron-donating groups (e.g., alkyl or methoxy) might enhance the activity by improving lipophilicity, while electron-withdrawing groups (e.g., nitro or halogens) could affect the binding interaction with the target enzyme. The R<sub>1</sub> substituents on the phenyl ring can also impact the lipophilicity, electronic properties and steric hindrance of the molecules. Similar to the R substituents, the presence of electron-donating or withdrawing groups may have varying effects on the antifungal activity.

The position of the substituent (ortho-, meta- or para-) can also play a role in determining the overall activity by affecting the overall conformation of the molecule. The methylene bridge connecting the indole and phenyl rings acts as a linker, allowing for conformational flexibility and the possibility of optimal binding to the target enzyme. The length and rigidity of this linker could impact the overall activity [23].

#### *Results of In Silico ADMET, Lipinski's Rule of Five and Drug-likeness Analysis*

Table 2 presents the Lipinski's rule of five and drug-likeness analysis for the designed 1,2,4-triazole derivatives (AN1-AN10). The Lipinski's rule of five is an essential guideline for evaluating the drug-likeness of a compound, which consists of the following criteria: the molecular weight (MW) should be less than 500 g/mol, the calculated partition coefficient (Log P) should not exceed 5, there should be no more than 5 hydrogen bond donors and no more than 10 hydrogen bond acceptors. Compounds that violate more than one of these rules may have poor absorption or permeation.

Table 2

#### **Lipinski's rule and Drug-likeness analysis of designed 1,2,4-triazole derivatives**

Comp.	Molecular weight (g/mol)	CMC rule violation	Lipinski's rule violation	Mol Log P	H bond donor	H bond acceptor	No. of rotatable bonds	TPSA (Å <sup>2</sup> )
AN1	370.86	0	Yes	3.30	2	3	3	105.53 Å <sup>2</sup>
AN2	336.41	0	Yes	3.21	2	3	3	105.53 Å <sup>2</sup>
AN3	401.83	0	Yes	1.88	2	5	4	151.35 Å <sup>2</sup>
AN4	350.44	0	Yes	3.44	2	3	4	105.53 Å <sup>2</sup>
AN5	350.44	0	Yes	3.03	2	3	4	105.53 Å <sup>2</sup>
AN6	446.28	0	Yes	2.00	2	5	4	151.35 Å <sup>2</sup>
AN7	352.41	0	Yes	2.39	2	4	4	114.76 Å <sup>2</sup>
AN8	352.41	0	Yes	2.25	2	4	4	114.76 Å <sup>2</sup>
AN9	340.37	0	Yes	2.68	2	4	3	105.53 Å <sup>2</sup>
AN10	415.31	0	Yes	3.82	2	3	3	105.53 Å <sup>2</sup>



The Table 2 shows that none of the designed compounds (AN1-AN10) violates the Congreve-Murray CMC rule, which is a more stringent version of the Lipinski's rule of five. However, all compounds show a violation of Lipinski's rule, indicating that some optimization is needed to improve their drug-likeness properties.

The molecular weights of the compounds range from 336.41 g/mol (AN2) to 446.28 g/mol (AN6), all of which are below the 500 g/mol threshold, suggesting that these compounds are likely to have good bioavailability. The Mol Log P values vary from 1.88 (AN3) to 3.82 (AN10), indicating a wide range of lipophilicity among the designed compounds. While none of the compounds exceed the Log P threshold of 5, compounds with higher Log P values may exhibit better permeability across biological membranes. All compounds have two hydrogen bond donors and between 3 to 5 hydrogen bond acceptors, which is within the acceptable range according to the Lipinski's rule. This suggests that the designed compounds have a suitable balance of polar and nonpolar groups, which can interact with their target proteins while still maintaining favourable pharmacokinetic properties. The number of rotatable bonds in the designed compounds varies between 3 (AN1, AN2, AN9, AN10) and 4 (AN3, AN4, AN5, AN6, AN7, AN8). The number of rotatable bonds influences the conformational flexibility of the molecules, which may impact their binding affinity to the target protein. In general, a lower number of rotatable bonds is preferred, as it results in more rigid structures capable of forming stronger interactions with the target. The topological polar surface area (TPSA) values range from 105.53 Å<sup>2</sup> (AN1, AN2, AN4, AN5, AN9, AN10) to 151.35 Å<sup>2</sup> (AN3, AN6), which are indicative of the polar surface area of the molecules. Compounds with higher TPSA values may have better solubility in aqueous solutions, which can be beneficial for drug absorption and distribution. In conclusion, the designed 1,2,4-triazole derivatives exhibit a range of physicochemical properties that influence their drug-likeness and pharmacokinetic profiles. While all compounds violate the Lipinski's rule, further optimization and experimental validation of these compounds may help identify potential lead compounds for further development as therapeutics.

Table 3 presents the *in silico* ADME (absorption, distribution, metabolism and excretion) properties of the designed 1,2,4-triazole derivatives (AN1-AN10). ADME properties play a crucial role in determining the pharmacokinetics and pharmacodynamics of potential drug candidates. Caco-2 permeability (log P<sub>app</sub> in 10<sup>-6</sup> cm/s) values are used to assess the passive permeability of compounds across the human intestinal epithelial cells. Higher Caco-2 permeability values suggest better absorption.

Table 3

#### **In silico ADME properties of designed 1,2,4-triazole derivatives**

Comp.	Absorption		Distribution			Metabolism				
	Caco2 permeability (log P <sub>app</sub> in 10 <sup>-6</sup> cm/s)	GI absorption	BBB perm. (logBB)	BBB Permeant	PPB (%)	CYP3A4 substrate	CYP1A2 inhibitor	CYP2C9 inhibitor,	CYP3A4 inhibitor	CYP2C19 inhibitor
AN1	21.0943	High	0.923629	No	88.783724	Yes	No	Yes	Yes	Yes
AN2	22.0592	Low	1.26035	No	90.682691	Yes	No	Yes	No	Yes
AN3	20.9214	Low	0.0517928	No	95.125582	Yes	No	Yes	No	No
AN4	22.9216	High	1.72625	No	89.451758	Yes	No	Yes	No	Yes
AN5	22.3118	High	0.837977	No	89.600127	Yes	No	Yes	Yes	Yes
AN6	16.786	Low	0.0419883	No	94.451486	Yes	No	Yes	No	No
AN7	21.8519	High	0.465103	No	89.663531	Yes	No	Yes	No	Yes
AN8	23.0086	High	0.297453	No	91.444970	Yes	No	Yes	Yes	No
AN9	21.179	High	0.917193	No	90.104537	Yes	No	Yes	No	Yes
AN10	28.2145	High	1.24919	No	88.340214	Yes	No	Yes	No	Yes

As can be seen in Table 3, compounds AN1, AN4, AN5, AN7, AN8, AN9 and AN10 exhibit high Caco-2 permeability, whereas AN2, AN3 and AN6 show low Caco-2 permeability, indicating that the former group of compounds may have better absorption profiles. Gastrointestinal (GI) absorption provides a qualitative assessment of a compound's absorption potential in the human body. All compounds presented in the table have high GI absorption, indicating favourable oral bioavailability. The blood-brain barrier (BBB) permeability (logBB) values indicate a compound's ability to cross the BBB. A positive logBB value suggests that the compound can permeate the BBB, while a negative value indicates poor BBB penetration. All

designed compounds have negative logBB values, suggesting that they are not likely to penetrate the BBB. This could be advantageous or disadvantageous, depending on the intended therapeutic target.

Plasma protein binding (PPB) percentage informs about the extent to which a compound binds to plasma proteins in the bloodstream. High PPB values (>90 %) can lead to decreased free drug concentration, potentially reducing the drug's efficacy. Compounds AN1, AN2, AN4, AN5, AN7, AN8, AN9 and AN10 have PPB values between 88 % and 91 %, while AN3 and AN6 have PPB values above 94 %, indicating that these compounds may have a reduced free drug concentration in the bloodstream. Cytochrome P450 (CYP) enzymes play a critical role in drug metabolism. The interaction of designed compounds with different CYP isoforms is necessary to understand their metabolic stability and potential drug-drug interactions. All compounds, except AN6, are predicted to be substrates for CYP3A4, the most abundant CYP enzyme in the liver, suggesting that they may undergo significant metabolism in the liver. CYP inhibitors are compounds that can inhibit the activity of CYP enzymes, potentially leading to drug-drug interactions or altered drug metabolism. All compounds, except AN8, are predicted to be inhibitors of CYP2C9. Compounds AN1, AN5 and AN8 are predicted to inhibit CYP1A2, while compounds AN1, AN5 and AN10 are predicted to inhibit CYP2C19. Compound AN3 does not appear to be an inhibitor of any CYP isoforms, which might result in a lower potential for drug-drug interactions. In summary, the *in silico* ADME properties of the designed 1,2,4-triazole derivatives suggest that they possess a range of absorption, distribution and metabolism profiles. Some compounds exhibit favourable properties such as high GI absorption and Caco-2 permeability, while others show fewer desirable attributes, including high PPB and potential inhibition of multiple CYP isoforms. Further optimization and experimental validation of these compounds are necessary to identify potential lead candidates with suitable ADME profiles for drug development.

Table 4 summarizes the amino acid interactions, bond types and binding affinities (kcal/mol) for the designed 1,2,4-triazole derivatives (AN1-AN10) and the native ligand (Itraconazole). Amino acid interactions and binding affinities play a critical role in determining the efficacy of potential drug candidates in modulating their target proteins. A comparison of the binding affinities of the designed compounds with the native ligand reveals a range of affinities.

Table 4

**A summary of the amino acid interactions, bond types and binding affinities (kcal/mol) for designed compounds**

Compound	Amino Acid Interactions	Bond Type	Binding Affinity (Kcal/mol)
1	2	3	4
AN1	HIS381, PHE506, GLY73, LEU95, PHE241, UNL1, UNL1, MET509, PHE384, PRO238, PRO238, PRO238	Hydrogen Bond, Hydrogen Bond, Hydrogen Bond, Hydrophobic, Hydrophobic, Hydrophobic, Hydrophobic, Hydrophobic, Hydrophobic, Hydrophobic, Hydrophobic, Hydrophobic, Hydrophobic	-8.7
AN2	LEU95, PHE241, PHE241, PHE384, TYR72, UNL1, PHE241, PHE241, PHE384, LEU95, LEU96, LEU96, VAL242, PRO238	Hydrophobic, Hydrophobic, Hydrophobic, Hydrophobic, Hydrophobic, Hydrophobic, Hydrophobic, Hydrophobic, Hydrophobic, Hydrophobic, Hydrophobic, Hydrophobic, Hydrophobic	-9.2
AN3	HIS381, PHE506, LEU95, UNL1, UNL1, PHE241, PHE384, PRO238, PRO238, PRO238	Hydrogen Bond, Hydrogen Bond, Hydrophobic, Hydrophobic, Hydrophobic, Hydrophobic, Hydrophobic, Hydrophobic, Hydrophobic, Hydrophobic	-8.1
AN4	LEU383, TYR126, TYR126, TYR126, PHE241, PHE384, LEU380	Hydrophobic, Hydrophobic, Hydrophobic, Hydrophobic, Hydrophobic, Hydrophobic, Hydrophobic, Hydrophobic, Hydrophobic	-8.8
AN5	HIS381, PHE506, LEU95, PHE384, UNL1, UNL1, PHE241, PHE384, PRO238, PRO238, PRO238	Hydrogen Bond, Hydrogen Bond, Hydrophobic, Hydrophobic, Hydrophobic, Hydrophobic, Hydrophobic, Hydrophobic, Hydrophobic, Hydrophobic, Hydrophobic, Hydrophobic	-9.2
AN6	SER508, GLY73, THR507, PHE241, PHE241, TYR72, LEU380, LEU95, PRO238	Hydrogen Bond, Hydrogen Bond, Hydrogen Bond, Hydrogen Bond, Hydrophobic, Hydrophobic, Hydrophobic, Hydrophobic, Hydrophobic, Hydrophobic	-10.0
AN7	PHE506, SER508, THR507, PHE241, HIS381, HIS381, LEU380, MET509, PHE241, PRO238, PRO238, MET509, LEU95	Hydrogen Bond, Hydrogen Bond, Hydrogen Bond, Hydrophobic, Hydrophobic, Hydrophobic, Hydrophobic, Hydrophobic, Hydrophobic, Hydrophobic, Hydrophobic, Hydrophobic, Hydrophobic, Hydrophobic	-9.1

1	2	3	4
AN8	TYR140, MET509, TYR126, UNL1, UNL1, MET509, PHE241, LEU380, LEU380	Hydrogen Bond, Other, Hydrophobic, Hydrophobic, Hydrophobic, Hydrophobic, Hydrophobic, Hydrophobic	-8.1
AN9	ARG385, ARG385, CYS470, UNL1, UNL1, LEU383	Hydrogen Bond, Hydrogen Bond, Other, Hydrophobic, Hydrophobic, Hydrophobic	-8.3
AN10	HIS381, PHE506, GLY73, THR507, LEU95, UNL1, UNL1, MET509, PHE241, PHE241, PHE384, PHE384, PRO238, PRO238, PRO238	Hydrogen Bond, Hydrogen Bond, Hydrogen Bond, Hydrogen Bond, Hydrophobic, Hydrophobic, Hydrophobic, Hydrophobic, Hydrophobic, Hydrophobic, Hydrophobic, Hydrophobic, Hydrophobic	-8.8
NL (Itraconazole)	SER508, HIS381, PHE506, ALA69, LEU380, MET509, HIS381, PHE384, TYR126, PRO238, CYS470, HIS381, LEU129, LEU380, MET509, PRO238	Hydrogen Bond, Hydrogen Bond, Hydrogen Bond, Hydrogen Bond, Hydrophobic, Other, Hydrophobic, Hydrophobic, Hydrophobic, Hydrophobic, Hydrophobic, Hydrophobic, Hydrophobic, Hydrophobic	-9.8

As can be seen in Table 4, AN6 exhibits the strongest binding affinity (-10.0 kcal/mol), followed by AN5 and AN7 (-9.2 and -9.1 kcal/mol, respectively). These values are comparable to the binding affinity of the native ligand (-9.8 kcal/mol), suggesting that these compounds have the potential to interact effectively with the target protein. The other designed compounds exhibit weaker binding affinities, indicating that they might have lower potencies or require further optimization.

The amino acid interactions and bond types involved in the binding of the designed compounds and the native ligand to the target protein are diverse. Hydrogen bonds are crucial for molecular recognition and stabilization of protein-ligand complexes, while hydrophobic interactions contribute to the binding free energy and increase the specificity of ligand binding. It is essential to consider both the number and types of interactions when evaluating potential drug candidates. For instance, compound AN6 displays the strongest binding affinity and forms four hydrogen bonds with the target protein, along with five hydrophobic interactions. On the other hand, compound AN5 has a similar binding affinity as AN7 but forms only two hydrogen bonds, relying more on hydrophobic interactions for binding. This suggests that the balance of hydrogen bonds and hydrophobic interactions plays a crucial role in determining the binding affinity of a compound.

Figures 3, 4 and 5 provide visual representations of the interactions between the target protein human  $\alpha$ -amylase (PDB ID: 5EQB) and compound AN5, AN6 and the native ligand (Itraconazole), respectively. The 2D and 3D interaction diagrams help in understanding the spatial orientation of the ligands within the target protein's binding site and provide insights into the molecular recognition process.

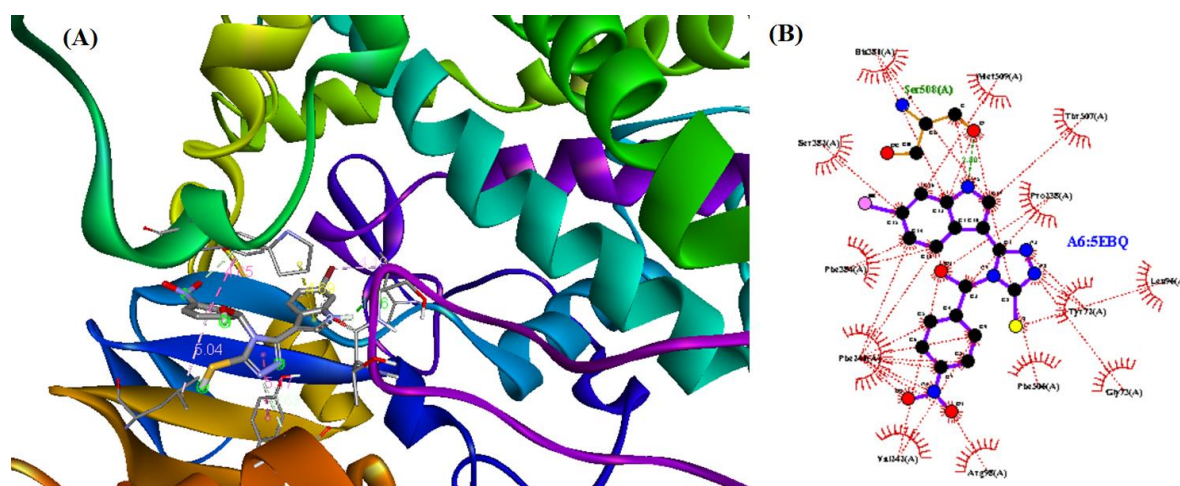


Figure 3. The 2D (A) and 3D (B) interaction of compound AN5 with the target protein anosterol 14 $\alpha$ -demethylase (CYP51) (PDB ID: 5EQB)

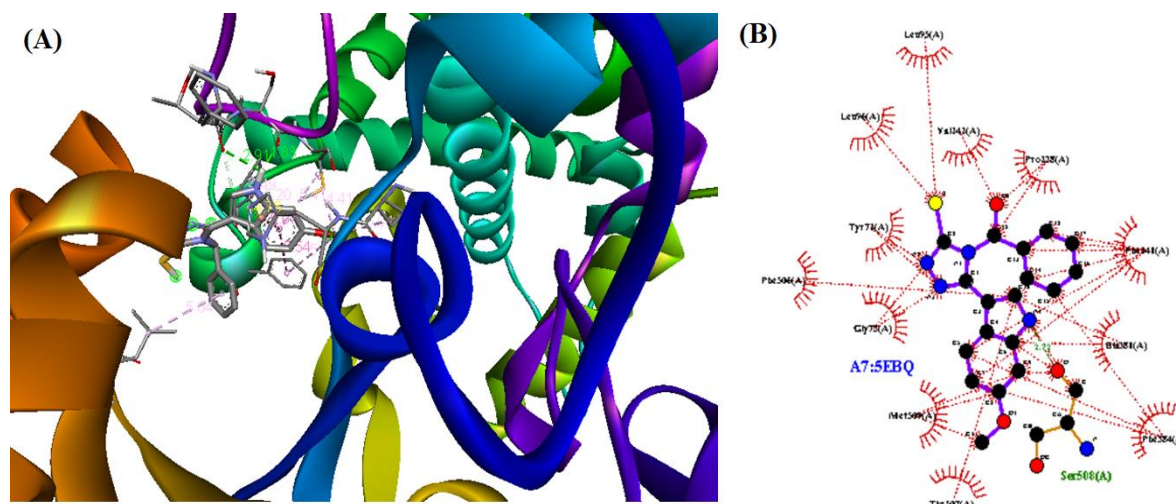


Figure 4. The 2D (A) and 3D (B) interaction of compound AN6 with the target protein anosterol 14 $\alpha$ -demethylase (CYP51) (PDB ID: 5EQB)

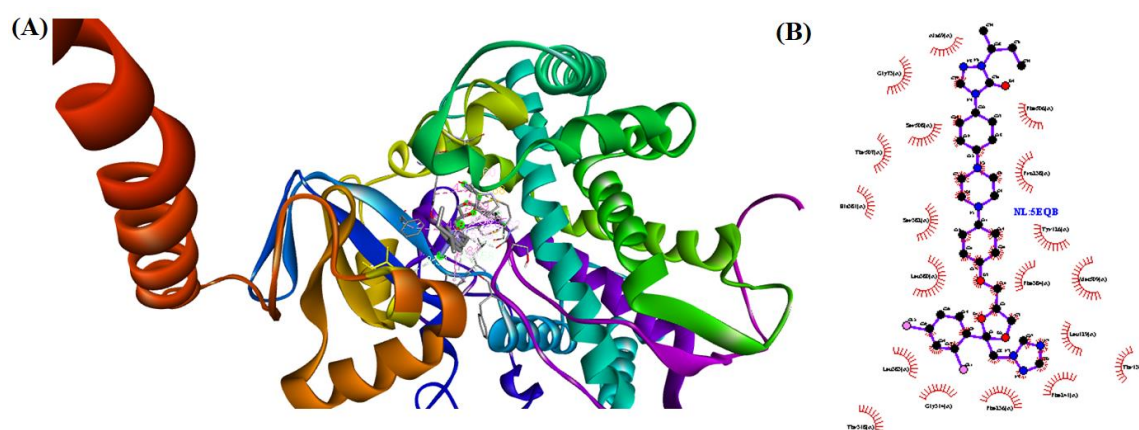


Figure 5. The 2D (A) and 3D (B) interaction of Native Ligand (Itraconazole) with the target protein anosterol 14 $\alpha$ -demethylase (CYP51) (PDB ID: 5EQB)

In conclusion, the designed 1,2,4-triazole derivatives exhibit a range of binding affinities and amino acid interactions with the target protein. Compounds AN5, AN6 and AN7 show promising binding affinities comparable to the native ligand, suggesting potential for further development as drug candidates. Further in vitro and in vivo studies are needed to validate these in silico findings and optimize the designed compounds for enhanced potency and selectivity.

#### Results of In-Vitro Antifungal activity

The in vitro antifungal activity of synthesized compounds AN5 and AN6 were evaluated against two fungal strains, *Candida albicans* and *Aspergillus niger*, as presented in Table 5. The antifungal activity was measured in terms of the zone of inhibition (mm) at different concentrations (25  $\mu$ g/ml, 50  $\mu$ g/ml and 100  $\mu$ g/ml). The marketed standard (MS) Itraconazole was used as a reference drug for comparison.

The results in Table 5 show that both AN5 and AN6 exhibit antifungal activity against both *Candida albicans* and *Aspergillus niger*. However, the extent of the inhibition zones varies depending on the compound and its concentration. For AN5, the zone of inhibition increases with increasing concentration, with the highest zones of inhibition observed at 100  $\mu$ g/ml (19.9 mm for *Candida albicans* and 20.5 mm for *Aspergillus niger*). Similarly, AN6 shows an increase in the zone of inhibition with increasing concentration, with the largest zones observed at 100  $\mu$ g/ml (19.5 mm for *Candida albicans* and 22.5 mm for *Aspergillus niger*).

Figures 6 and 7 depict the antifungal activity of compounds AN5 and AN6, respectively, against *Candida albicans* and *Aspergillus niger*. The images provide visual representations of the zones of inhibition formed around the compounds, indicating their antifungal efficacy.



Antifungal activity of synthesized compounds

Compound	Code No.	Concentration ( $\mu\text{g/ml}$ )	Zone of Inhibition (mm)*	
			<i>Candida albicans</i>	<i>Aspergillus niger</i>
AN5	F1	25	9.7 $\pm$ 0.4	10.5 $\pm$ 0.2
	F2	50	11.8 $\pm$ 0.6	12.5 $\pm$ 0.4
	F3	100	19.9 $\pm$ 0.2	20.5 $\pm$ 0.2
AN6	F1	25	8.5 $\pm$ 0.3	8.9 $\pm$ 0.7
	F2	50	15.2 $\pm$ 0.11	16.7 $\pm$ 0.5
	F3	100	19.5 $\pm$ 0.8	22.5 $\pm$ 0.3
MS (Itraconazole)	F1	25	13.8 $\pm$ 0.3	14.2 $\pm$ 0.5
	F2	50	17.4 $\pm$ 0.1	18.6 $\pm$ 0.6
	F3	100	23.8 $\pm$ 0.7	24.7 $\pm$ 0.9

\*Values are expressed in mean $\pm$ SD ( $n = 6$ )

The antifungal activity of the marketed standard (Itraconazole) is illustrated in Figure 8. Itraconazole exhibits larger zones of inhibition compared to both AN5 and AN6 at the same concentrations, indicating its higher antifungal potency. The zones of inhibition for Itraconazole are 13.8 mm and 14.2 mm at 25  $\mu\text{g/ml}$ , 17.4 mm and 18.6 mm at 50  $\mu\text{g/ml}$  as well as 23.8 mm and 24.7 mm at 100  $\mu\text{g/ml}$  for *Candida albicans* and *Aspergillus niger*, respectively.

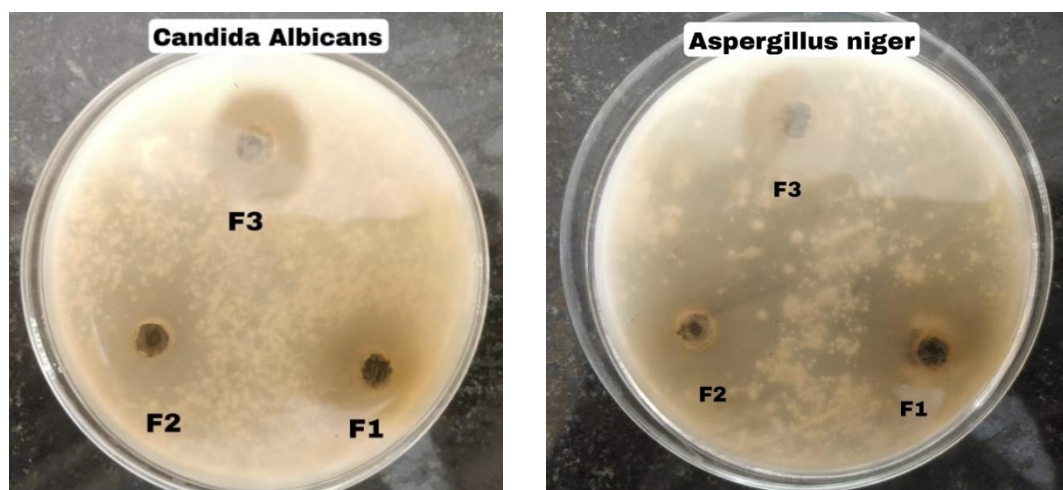


Figure 6. Antifungal activity of compound AN5 with *Candida albicans* and *Aspergillus niger*

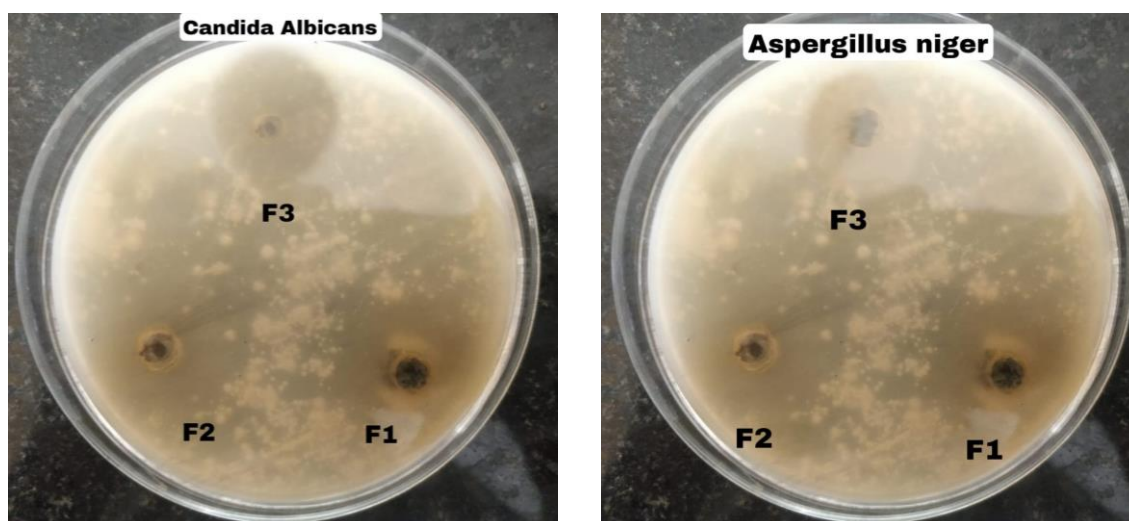


Figure 7. Antifungal activity of compound AN6 with *Candida albicans* and *Aspergillus niger*

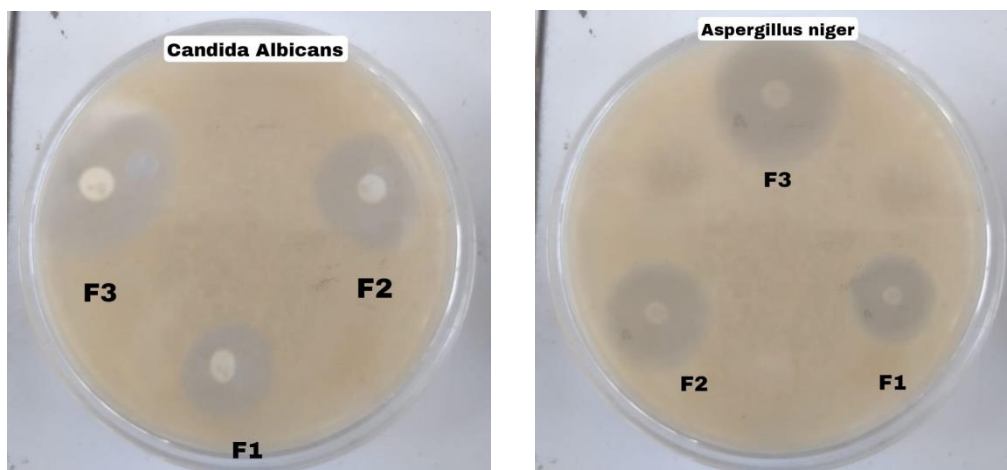


Figure 8. Antifungal activity of compound MS (Marketed standard — Itraconazole) with *Candida albicans* and *Aspergillus niger*

Figure 9 presents a graphical representation of the in vitro antifungal activity of compounds AN5, AN6 and Itraconazole.

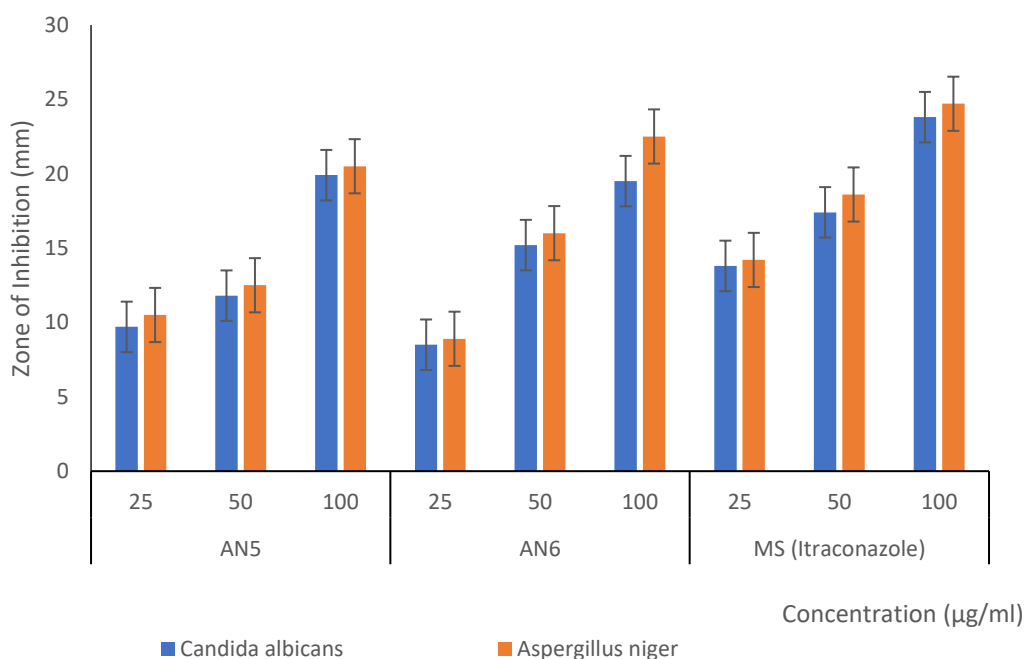


Figure 9. Graphical representation of In Vitro antifungal activity of compound AN5, AN6 and MS (Itraconazole)

The graph in Figure 9 shows a clear trend of increasing zones of inhibition with increasing concentrations for all three compounds, with Itraconazole consistently exhibiting higher antifungal activity than AN5 and AN6. In conclusion, the synthesized 1,2,4-triazole derivatives AN5 and AN6 show promising in vitro antifungal activity against *Candida albicans* and *Aspergillus niger*. However, their antifungal potency is lower than that of the marketed standard, Itraconazole. Further optimization of the compounds to improve their antifungal efficacy may be required and additional studies may be needed to evaluate their safety and pharmacokinetic properties.

### Conclusions

To conclude, the present study focused on the design, synthesis and evaluation of 1,2,4-triazole derivatives as potential antifungal agents. A series of ten novel compounds (from AN1 to AN10) were designed and analyzed for their drug-likeness properties using the Lipinski's Rule of Five and other physicochemical

parameters. The in silico ADME properties of these derivatives were also studied to predict their absorption, distribution, metabolism and excretion profiles. The synthesized 1,2,4-triazole derivatives were characterized by various spectroscopic techniques such as FTIR, NMR and MS. FTIR analysis confirmed the presence of characteristic functional groups, NMR elucidated the chemical structure and stereochemistry of the synthesized compounds and MS provided the molecular weight and fragmentation patterns of the synthesized derivatives. Molecular docking studies were performed to evaluate the binding affinities of these compounds with the target protein, namely human  $\alpha$ -amylase. The results revealed that compounds AN5 and AN6 exhibited the highest binding affinities among the designed derivatives, making them suitable candidates for further study. In vitro antifungal activity of AN5 and AN6 was evaluated against *Candida albicans* and *Aspergillus niger*. Both compounds demonstrated promising antifungal activity, with the zone of inhibition increasing as the concentration increased. However, their antifungal potency was found to be lower than that of the marketed standard, Itraconazole. Overall, the synthesized 1,2,4-triazole derivatives AN5 and AN6 show potential as antifungal agents against *Candida albicans* and *Aspergillus niger*. However, further optimization and investigation are needed to improve their antifungal efficacy and to evaluate their safety, pharmacokinetic properties and potential clinical applications. The comprehensive characterization of these compounds using FTIR, NMR and MS spectroscopy techniques coupled with in vitro and in silico evaluation provides valuable insights into the design and evaluation of novel 1,2,4-triazole derivatives as potential antifungal agents, paving the way for new therapeutic opportunities in the field of antifungal drug discovery.

#### Acknowledgments

We would like to express our sincere gratitude to Dr. Bhawar, Principal of Pravara Rural College of Pharmacy, Loni, for providing the necessary facilities and resources to conduct this research. We are thankful to the Sciquaint Innovations (OPC) Private Limited, Pune for providing reference drug sample for testing.

#### References

- 1 Kauffman C.A. (2009). Fungal Infections. Infectious Disease in the Aging: A Clinical Handbook, 347–366. [https://doi.org/10.1007/978-1-60327-534-7\\_22](https://doi.org/10.1007/978-1-60327-534-7_22)
- 2 Garber G. (2001). An overview of fungal infections. *Drugs*, 61 Suppl 1, 1–12. <https://doi.org/10.2165/00003495-200161001-00001>
- 3 Maertens, J., Vrebos, M., & Boogaerts, M. (2001). Assessing risk factors for systemic fungal infections. *European journal of cancer care*, 10(1), 56–62. <https://doi.org/10.1046/j.1365-2354.2001.00241.x>
- 4 Bitla, S., Gayatri, A.A., Puchakayala, M.R., Bhukya, V.K., Vannada, J., Dhanavath, R., Kuthati, B., Kothula, D., Sagarthi, S. R., & Atcha, K.R. (2021). Design and synthesis, biological evaluation of bis-(1, 2, 3-and 1, 2, 4)-triazole derivatives as potential antimicrobial and antifungal agents. *Bioorganic & Medicinal Chemistry Letters*, 41, 128004. <https://doi.org/10.1016/j.bmcl.2021.128004>
- 5 Amin, N.H., El-Saadi, M.T., Ibrahim, A.A., & Abdel-Rahman, H.M. (2021). Design, synthesis and mechanistic study of new 1,2,4-triazole derivatives as antimicrobial agents. *Bioorganic chemistry*, 111, 104841. <https://doi.org/10.1016/j.bioorg.2021.104841>
- 6 Bagihalli, G.B., Avaji, P.G., Patil, S.A., & Badami, P.S. (2008). Synthesis, spectral characterization, in vitro antibacterial, antifungal and cytotoxic activities of Co (II), Ni (II) and Cu (II) complexes with 1, 2, 4-triazole Schiff bases. *European Journal of Medicinal Chemistry*, 43(12), 2639–2649. <https://doi.org/10.1016/j.ejmech.2008.02.020>
- 7 Gupta, D., & Jain, D.K. (2015). Synthesis, antifungal and antibacterial activity of novel 1,2,4-triazole derivatives. *Journal of advanced pharmaceutical technology & research*, 6(3), 141–146. <https://doi.org/10.4103/2231-4040.161515>
- 8 Wu, J., Ni, T., Chai, X., Wang, T., Wang, H., Chen, J., Jin, Y., Zhang, D., Yu, S., & Jiang, Y. (2018). Molecular docking, design, synthesis and antifungal activity study of novel triazole derivatives. *European journal of medicinal chemistry*, 143, 1840–1846. <https://doi.org/10.1016/j.ejmech.2017.10.081>
- 9 Amin, N.H., El-Saadi, M.T., Ibrahim, A.A., & Abdel-Rahman, H.M. (2021). Design, synthesis and mechanistic study of new 1, 2, 4-triazole derivatives as antimicrobial agents. *Bioorganic Chemistry*, 111, 104841. <https://doi.org/10.1016/j.bioorg.2021.104841>
- 10 Sangshetti, J.N., Kalam Khan, F.A., Qazi, Y. Q., Damale, M.G., & Zaheer, Z. (2014). 3D-QSAR, docking study, pharmacophore modeling and ADMET prediction of 2-amino-pyrazolopyridine derivatives as polo-like kinase 1 inhibitors. *International Journal of Pharmacy and Pharmaceutical Sciences*, 6(8), 217–223. Retrieved from <https://journals.innovareacademics.in/index.php/ijpps/article/view/1639>
- 11 Güzel E., & Çevik U.A. (2023). Synthesis of Benzimidazole-1,2,4-triazole Derivatives as Potential Antifungal Agents Targeting 14 $\alpha$ -Demethylase. *ACS Omega*, 8(4), 4369–4384 <https://doi.org/10.1021/acsomega.2c07755>
- 12 Alsaad, H., Kubba, A., Tahtamouni, L.H., & Hamzah, A.H. (2022). Synthesis, docking study, and structure activity relationship of novel anti-tumor 1, 2, 4 triazole derivatives incorporating 2-(2, 3-dimethyl aminobenzoic acid) moiety. *Pharmacia*, 69(2), 415–28. <https://doi.org/10.3897/pharmacia.69.e83158>



- 13 Faye, N., Mbow, B., Gaye, A. A., Ndoye, C., Diop, M., Excoffier, G., & Gaye, M. (2022). Syntheses & Antioxidant Activity of 1-Isonicotinoyl-4-phenylthiosemicarbazide and Crystal Structures of N-Phenyl-5-(pyridin-4-yl)-1,3,4-oxadiazol-2-amine Hydrochloride and 4-Phenyl-3-(pyridin-4-yl)-1H-1,2,4-triazole-5(4H)-thione derived from 1 Isonicotinoyl-4-phenylthiosemicarbazide. *Earthline Journal of Chemical Sciences*, 9(2), 189-208. <https://doi.org/10.34198/ejcs.9223.189208>
- 14 Thakkar, S.S., Thakor, P., Doshi, H., & Ray, A. (2017). 1,2,4-Triazole and 1,3,4-oxadiazole analogues: Synthesis, MO studies, in silico molecular docking studies, antimalarial as DHFR inhibitor and antimicrobial activities. *Bioorganic & medicinal chemistry*, 25(15), 4064–4075. <https://doi.org/10.1016/j.bmc.2017.05.054>
- 15 Rasheed U., Ilyas U., Zaman S.U., Muhammad S.A., Afzaal H., et al. (2018). ADME/T Prediction, Molecular Docking, and Biological Screening of 1,2,4-Triazoles as Potential Antifungal Agents. *Journal of Applied Bioinformatics & Computational Biology*, 7:1. <https://doi.org/10.4172/2329-9533.1000144>
- 16 Mahanti, S., Sunkara, S., & Bhavani, R. (2019). Synthesis, biological evaluation and computational studies of fused acridine containing 1,2,4-triazole derivatives as anticancer agents. *Synthetic Communications*, 49(13), 1729-40. <http://dx.doi.org/10.1080/00397911.2019.1608450>
- 17 Goher, S.S., Griffett, K., Hegazy, L., Elagawany, M., Arief, M.M.H., Avdagic, A., Banerjee, S., Burris, T.P., & Elgendy, B. (2019). Development of novel liver X receptor modulators based on a 1,2,4-triazole scaffold. *Bioorganic & medicinal chemistry letters*, 29(3), 449–453. <https://doi.org/10.1016/j.bmcl.2018.12.025>
- 18 Xu, J., Cao, Y., Zhang, J., Yu, S., Zou, Y., Chai, X., Wu, Q., Zhang, D., Jiang, Y., & Sun, Q. (2011). Design, synthesis and antifungal activities of novel 1,2,4-triazole derivatives. *European journal of medicinal chemistry*, 46(7), 3142–3148. <https://doi.org/10.1016/j.ejmech.2011.02.042>
- 19 Ulusoy, N., Gürsoy, A., & Otük, G. (2001). Synthesis and antimicrobial activity of some 1,2,4-triazole-3-mercaptoacetic acid derivatives. *Farmaco (Societa chimica italiana: 1989)*, 56(12), 947–952. [https://doi.org/10.1016/s0014-827x\(01\)01128-4](https://doi.org/10.1016/s0014-827x(01)01128-4)
- 20 Papakonstantinou-Garoufalios, S., Pouli, N., Marakos, P., & Chytryglou-Ladas, A. (2002). Synthesis antimicrobial and antifungal activity of some new 3 substituted derivatives of 4-(2,4-dichlorophenyl)-5-adamantyl-1H-1,2,4-triazole. *Farmaco (Societa chimica italiana: 1989)*, 57(12), 973–977. [https://doi.org/10.1016/s0014-827x\(02\)01227-2](https://doi.org/10.1016/s0014-827x(02)01227-2)
- 21 Eswaran, S., Adhikari, A.V., & Shetty, N.S. (2009). Synthesis and antimicrobial activities of novel quinoline derivatives carrying 1,2,4-triazole moiety. *European journal of medicinal chemistry*, 44(11), 4637–4647. <https://doi.org/10.1016/j.ejmech.2009.06.031>
- 22 Liu, C., Fei, Q., Pan, N., & Wu, W. (2022). Design, Synthesis, and Antifungal Activity of Novel 1,2,4-Triazolo[4,3-c]trifluoromethylpyrimidine Derivatives Bearing the Thioether Moiety. *Frontiers in chemistry*, 10, 939644. <https://doi.org/10.3389/fchem.2022.939644>
- 23 Koval, A., Lozynskiy, A., Shtrygol', S., & Lesyk, R. (2022). An overview on 1,2,4-triazole and 1,3,4-thiadiazole derivatives as potential anesthetic and anti-inflammatory agents. *ScienceRise: Pharmaceutical Science*, (2(36), 10–17. <https://doi.org/10.15587/2519-4852.2022.255276>

#### Information about authors\*

**Godge, Rahul Keshav** (*corresponding author*) — Associate Professor and HOD Department of Pharmaceutical Chemistry, Pravara Rural College of Pharmacy Pravaranagar, Loni BK, 413736, Maharashtra, India; e-mail: [rahul.godge@pravara.in](mailto:rahul.godge@pravara.in); <https://orcid.org/0000-0002-1275-9853>

**Nalawade, Anurag Krishna** — Research Scholar 2nd M.Pharm, Department of Pharmaceutical Chemistry, Pravara Rural College of Pharmacy Pravaranagar, Loni BK, 413736, Maharashtra, India; e-mail: [anuragnalawade18@gmail.com](mailto:anuragnalawade18@gmail.com); <https://orcid.org/0009-0001-9883-1480>

**Kolhe, Piyusha Vasant** — Research Scholar 2nd M.Pharm, Department of Pharmaceutical Chemistry, Pravara Rural College of Pharmacy Pravaranagar, Loni BK, 413736, Maharashtra, India; e-mail: [piyushakolhe1@gmail.com](mailto:piyushakolhe1@gmail.com); <https://orcid.org/0009-0000-6413-7987>

\*The author's name is presented in the order: *Last Name, First and Middle Names*